Received: 3 June 2021 | Accepted: 18 December 2021

DOI: 10.1111/srt.13139

ORIGINAL ARTICLE

WILEY

Differential diagnosis of basal cell carcinoma by high-resolution ultrasound elastography

Xiaohua Han[1] | Jiyou Li[1] | Fuqiang Zeng[1] | Hongmei Liu[2] | Yanni He[2]

[1] Department of Ultrasound, Zhongshan Hospital of Traditional Chinese Medicine, Zhongshan, China

[2] Department of Ultrasound, Institute of Ultrasound in Musculoskeletal Sports Medicine, Guangdong Second Provincial General Hospital, Guangzhou, China

Correspondence
Jiyou Li, Department of Ultrasound, Zhongshan Hospital of Traditional Chinese Medicine, Zhongshan, Guangdong 528400, China.
Email: 448430342@qq.com

Abstract

The aim of this study was to assess the value of high-resolution ultrasonic quantitative parameters of shear wave elastography (SWE) in basal cell carcinoma (BCC). A total of 86 cases of BCC were enrolled as the case group, and 38 other similar skin pigmented lesions were randomly selected as the control group. Using pathological results as the gold standard, the diagnostic test method was used to evaluate the ability of high-frequency ultrasonic elastography to diagnose BCC, and the 2D ultrasonographic features, blood flow image characteristics, and SWE of BCC were summarized.

KEYWORDS
BCC, SWE, ultrasound, Young's modulus

1 | INTRODUCTION

The global incidence of skin cancer has been steadily increasing in recent years. Its main risk factors are long-term day-light exposure to ultraviolet radiation, exposure to chemical carcinogens, radiation, and so on.[1] From 2015 to 2017, the average annual growth rate of the total number of patients with skin cancer was 14.67% in China. The Guangdong Province has the largest number of skin cancer patients, where the main occupation is farming.[2] Approximately one-fifth of the population in Belgium had skin cancer in 2014.[3] Skin cancer is a serious malignancy, and a global public health problem.

Basal cell carcinoma (BCC), squamous cell carcinoma, and melanoma are the most common types of skin cancer, among which BCC has the highest incidence.[4] BCC is the most difficult to distinguish from seborrheic keratosis and pigmented nevus because of their similar clinical manifestation. The examination of skin lesions depends upon the clinician's experience of visual observation or simple dermoscopy, which is only on the longitudinal level.[5,6] Even experienced clinicians find it difficult to distinguish BCC from seborrheic keratosis and pigmented nevus, especially early BCC.

The recent developments in high-resolution ultrasound (HRUS) have made skin ultrasound examination possible.[1,7–9] Mandava et al.[10] superficial skin lesions are very small, HRUS is the non-invasive test because which can effective resolution of the skin and the surrounding tissues, is the noninvasive test that can be used to evaluate superficial skin lesions because they are very small. They imaged skin lesions by 2D ultrasonography, but it is not easy for some atypical cases or young sonologists. Shear wave elastography (SWE) has been shown to be a powerful tool to estimate tissue stiffness.[11–15] There are numerous reports on the application of SWE in skin diseases.[16–19] The major type of BCC is solid cases, which involve palisade-like arrangement, so the texture is hard. The SWE has solidity measured values, which can help to identify useful imaging evidence for the differential diagnosis of BCC, in order to increase the reliability of the diagnosis and treatment.

2 | MATERIALS AND METHODS

2.1 | Design

This retrospective analysis was performed at the Zhongshan Hospital of Traditional Chinese Medicine between January 2018 and December 2020. A total of 124 patients (54 males and 70 females, mean age 55.2±23.4 years), including 86 BCC cases and 38 controls (29 cases with seborrheic keratosis and 9 cases with pigmented nevus), were included in the study. Cutaneous lesions with surface scab were excluded from the study. This study was approved by the Ethics

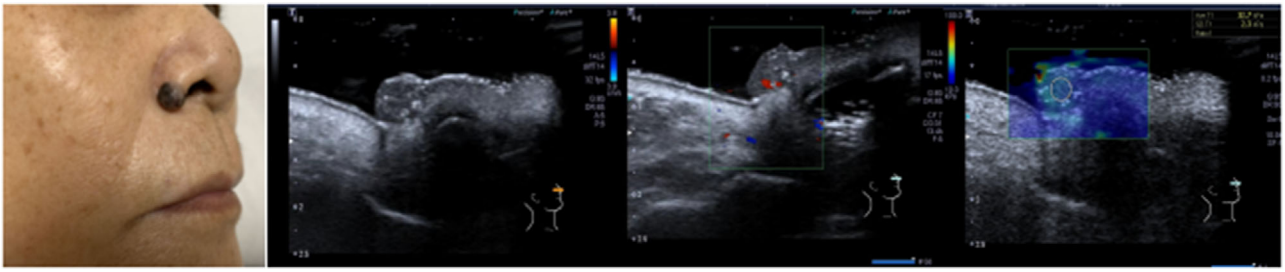

FIGURE 1 2D, Doppler, and SWE images of BCC

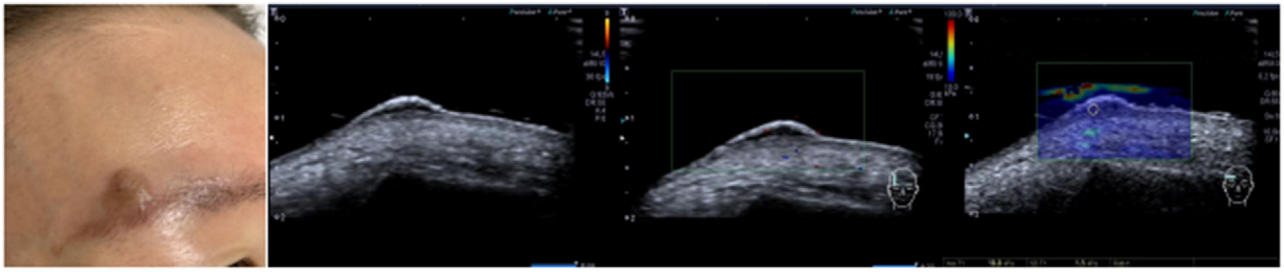

FIGURE 2 2D, Doppler, and SWE images of seborrheic keratosis

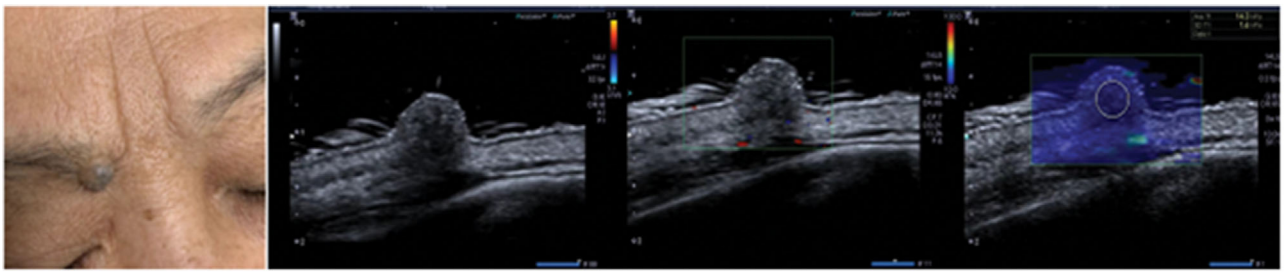

FIGURE 3 2D, Doppler, and SWE images of pigmented nevus

Commission of our hospital. All patients gave informed consent before examination.

2.2 | Ultrasonic imaging data acquisition

SWE was performed with an Apollo 500 ultrasound system (Canon, Japan), using a 15 MHz linear transducer (L10-15). In every participant, a thick coupling agent was placed between the transducer and the skin to improve docking. First, a thick coupling agent and vertical probe was placed to perform routine 2D ultrasonic imaging, wherein the structure of the epidermis, dermis, subcutaneous adipose layer, and surrounding soft tissue of the skin were clearly displayed, and the size, shape, internal echo, and the depth of the skin layer of the space-occupying lesion were observed. Next, the perfusion information was assessed by color Doppler ultrasound. Finally, all participants underwent a standardized protocol (placed the lesion at a same depth of about 10 mm for 3–5 s) that consisted of high-resolution ultrasonic imaging and SWE. After the image was stabilized and frozen, region of interest, which included as many lesion areas as possible, was selected, circular or elliptical, and Young's modulus was automatically measured three times by the software, and the mean of the three values calculated was used for analysis.

2.3 | Statistical analysis

Continuous variables were presented as mean ± standard deviation. All reported *p*-values were two-sided. A *p*-value < 0.05 was considered to be statistically significant. Statistical analysis was performed using SPSS version 22.0 (IBM Corp, Armonk, NY, USA). Comparisons between the BCC and control groups were made with one-way ANOVA.

3 | RESULTS

3.1 | Pathological types of skin lesions and high-frequency ultrasonic imaging

A total of 124 patients, with 86 BCC cases and 38 controls (29 cases with seborrheic keratosis and 9 cases with pigmented nevus), were

TABLE 1 Pathological types of skin lesions and ultrasonic imaging

	n	2D	Color Doppler (blood flow signals)	SWE(mean ± standard deviation)
BCC	86	Heterogeneous, Gravel calcifications Skin thickening, roughness, varying degrees of epidermal defects	More, dispersed	36.7 ±5.2 KPA
Seborrheic keratosis	29	Only present in the epidermis, no obvious changes in the dermis	Dendritic	19.6 ± 4.8 KPA
Pigmented nevus	9	Slightly higher than BBC, thicken of epidermis	Poor	23.6 ± 4.7 KPA

included in this study. BCC showed oval-shaped lesions, with skin thickening, roughness, or varying degrees of epidermal defects. Color blood flow signals are rich, and the blood vessels are dense and circuitous. Seborrheic keratosis showed cauliflower-like appearance in the reference group, and the lesions were only present in the epidermis, with no obvious changes in the dermis. Most of the color blood flow signals were abundant, but the blood flow was dendritic. The local defect appeared in the posterior dermis of seborrheic keratosis, but the edge was regular. The echo of pigmented nevus was slightly higher than that of BBC. There was little thicken in the anterior epidermis of pigmented nevus, and the blood flow signal was generally poor in lesion. 2D, color Doppler, and elastography images of BCC, seborrheic keratosis, and pigmented nevus are shown in Figures 1–3, Table 1. The mean Young's modulus of BCC, seborrheic keratosis, and pigmented nevus were 36.7 ±5.2 KPA, 19.6 ± 4.8 KPA, and 23.6 ± 4.7 KPA, respectively. There was significant difference in the mean value of Young's modulus between BCC and controls ($p < 0.05$, $F = 129.482$).

Ultrasonic graphic in the BCC and control groups is shown in Table 1.

Scatter plot of Young's modulus in the BCC and control groups is shown in Figure 4.

3.2 | Mean Young's modulus ROC curve, and diagnostic threshold of BCC and control group

Using pathological results as the gold standard, the diagnostic threshold of Young's modulus was obtained by ROC curve. The area under the ROC curve was 0.939, and the corresponding sensitivity and specificity were obtained (Figure 5). When the maximum area under ROC

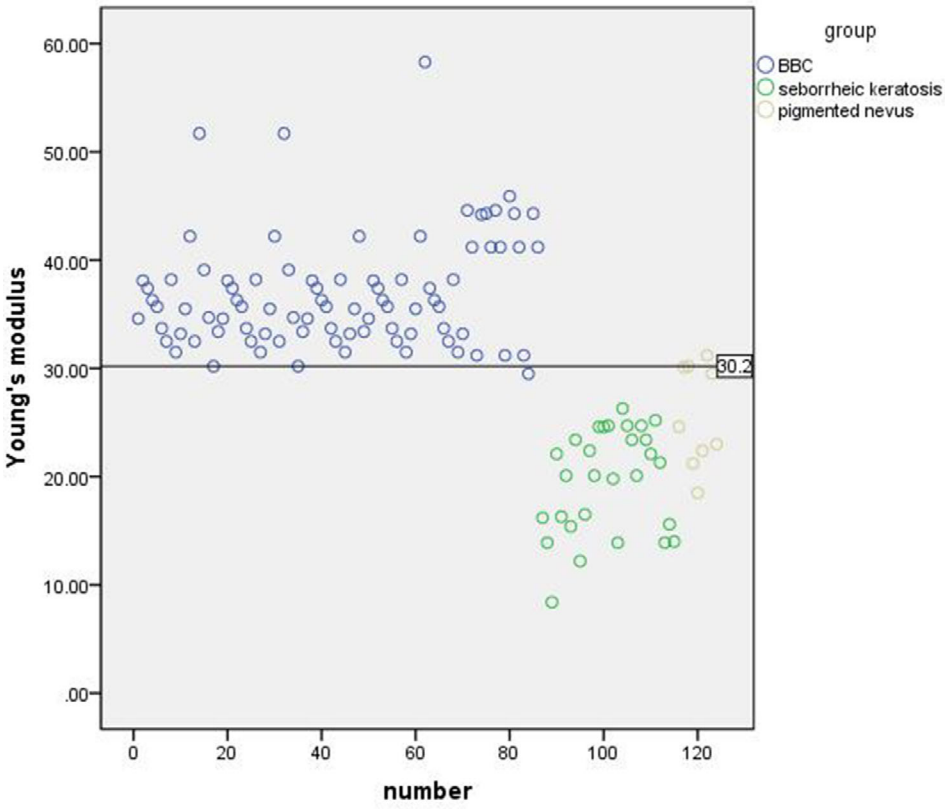

FIGURE 4 Scatter plot of 124 cases and its boundary value

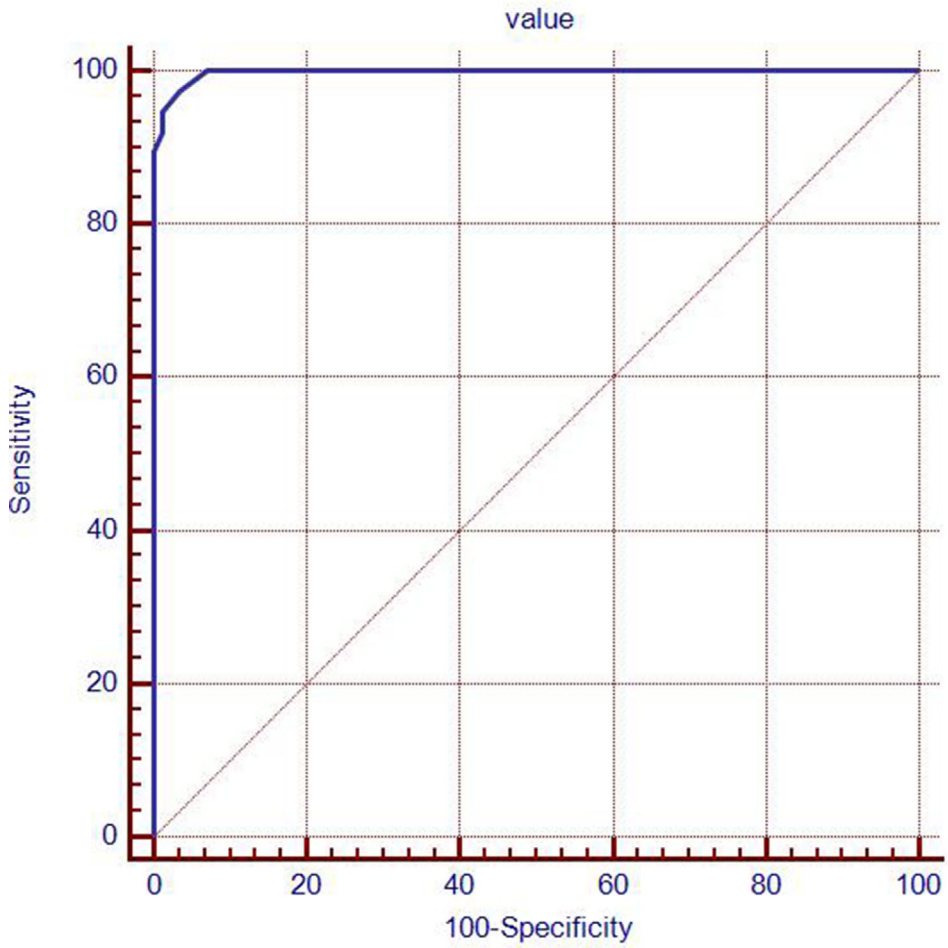

FIGURE 5 ROC curve for skin space-occupying lesions

curve was 0.939, the mean value of Young's modulus was 30.2 Kpa (BCC was > 30.2 Kpa and control group was <30.2 Kpa). The diagnostic sensitivity and specificity were 97.37% and 96.51%.

4 | DISCUSSION

The development of HRUS makes it possible to examine the skin by ultrasound, and the images of interest can be moved back with ultrasound pad or coated with a thick coupling agent to improve the near field resolution, and to clearly distinguish the epidermis and dermis of the skin.[8,10] Higher resolution is ideal for displaying the border and surrounding tissue of the lesion. In order to achieve high resolution and good reproducibility of elastography, we placed a thick coupling agent in front of the lesion, and the lesion was located about 10 mm in depth.

Color Doppler ultrasound can be used to evaluate the perfusion of the lesions, but the measurement of some superficial lesions is not adequately sensitive, as well as the blood supply cross-section of BCC and seborrheic keratosis. In 2002, elastography was proposed as a new technique for assessing tissue stiffness, and has been used in the diagnosis of liver, breast, testis, and thyroid lesions.[11–15] SWE can be used to measure the value of tissue elasticity and the absolute value of Young's modulus, through the quantitative analysis system. The larger the value, the harder is the lesion in the skin.[16–19] In this study, SWE was used to measure the absolute value of Young's modulus of skin lesions. No artificial pressure was needed in this process, so the influence of human factors was effectively avoided, especially in superficial skin lesions. Malignant lesions typically occur on the head and face, especially around the nasal alar. A certain thickness of coupling agent is placed in front of the lesion. The operation has good repeatability.

In this study, higher resolution is ideal for displaying the border and surrounding tissue of the lesion, which help to locate the layer. Color Doppler ultrasound is not adequately sensitive and specific. The ROC curve was used to obtain the optimal diagnostic threshold of Young's modulus and the corresponding sensitivity and specificity. The diagnostic threshold was > 30.2 KPA for BBC and <30.2 KPA for benign lesions. The diagnostic sensitivity and specificity were 97.37% and 96.51%, respectively. Although the specificity was not 100%, but combined with the 2D morphology and blood perfusion information, the nature of the lesion could be accurately diagnosed, and the diagnostic accuracy reached 100%. Since the number of cases and disease types in this study were not comprehensive, and only consisted of seborrheic

keratosis and pigmented nevus, which were difficult to diagnose from BCC, more comprehensive data will be collected and analyzed in the future.

In summary, the size, shape, internal echo, depth, and perfusion of the skin space-occupying lesions were clearly assessed by HRUS, and the hardness of the lesions was measured by SWE. With the accumulation of clinical experience, HRUS elastography will be beneficial for the clinical diagnosis and treatment of skin space-occupying lesions.

5 | CONCLUSION

High-frequency ultrasonic elastography has high differential diagnosis ability for BCC, which will help diagnosis BCC from seborrheic keratosis and pigmented nevus because of their similar clinical manifestation, especially early BCC.

REFERENCES

1. Covarelli P, Burini G, Barberini F, Caracappa D, Boselli C, Noya G, et al. The integrated role of ultrasonography in the diagnosis of soft tissue metastases from melanoma: preliminary report of a single-center experience and literature review. In Vivo. 2013;27:827–33.
2. Xu L, Zhang L, Tian X, Zhao Y, Miu Z, Xue M, et al. Epidemiological research on inpatients with skin cancer in China. Chin J Evid Based Med. 2020;20(11):1280–3.
3. Pil L, Hoorens I, Vossaert K, Kruse V, Tromme I, Speybroeck N, et al. Burden of skin cancer in Belgium and cost-effectiveness of primary prevention by reducing ultraviolet exposure. Prev Med. 2016,93:177–82.
4. Cho S, Kim MH, Whang KK, Hahm JH. Clinical and histopathological characteristics of basal cell carcinoma in Korean patients. J Dermatol. 1999;26(8):494–501.
5. Altamura D, Menzies SW, Argenziano G, Zalaudek I, Soyer HP, Sera F, et al. Dermatoscopy of basal cell carcinoma: morphologic variability of global and local features and accuracy of diagnosis. J Am Acad Dermatol. 2010;62:67–75.
6. Hong H, Sun J, Cai W. Anatomical and molecular imaging of skin cancer. Clin Cosmet Investig Dermatol. 2008;1:1–17.
7. Hayashi K, Koga H, Uhara H, Saida T. High-frequency 30-MHz sonography in preoperative assessment of tumor thickness of primary melanoma: usefulness in determination of surgical margin and indication for sentinel lymph node biopsy. Int J Clin Oncol. 2009;14:426–30.
8. Hinz T, Ehler LK, Hornung T, Voth H, Fortmeier I, Maier T, et al. Preoperative characterization of basal cell carcinoma comparing tumor thickness measurement by optical coherence tomography, 20-MHz ultrasound and histopathology. Acta Derm Venereol. 2012;92:132–37.
9. Chami L, Lassua N, Chebil M, Robert C. Imaging of melanoma: usefulness of ultrasonography before and after contrast injection for diagnosis and early evaluation of treatment. Clin Cosmet Investig Dermatol. 2011;4:1–6.
10. Mandava A, Ravuri PR, Konathan R. High-resolution ultrasound imaging of cutaneous lesions. Indian J Radiol Imaging. 2013;23:269–77.
11. Rubaltelli L, Corradin S, Dorigo A, Stabilito M, Tregnaghi A , Borsato S , et al. Differential diagnosis of benign and malignant thyroid nodules at elastosonography. Ultraschall Med. 2009;30:175–9.
12. Taljanovic MS, Gimber LH, Becker GW, Latt LD, Klauser AS, Melville DM, et al. Shear-wave elastography: basic physics and musculoskeletal applications. Radiographics. 2017;37:855–70.
13. Tianyi Z, Xuan Xu, Bing S, Guozhen Y, manman H, Shaochun W, et al. Detection and evaluation of testicular hardness in male infertility patients by real-time shear wave elastography. J Clin Ultrasound Med. 2018;20:614–7.
14. Changyue L, Ying Z, Jian Z, Fankun M. Real-time two-dimensional shear wave elastography non-invasive evaluation of liver fibrosis and its correlation with pathological staging. J Clin Ultrasound Med. 2018;20:518–20.
15. Sha YS, Yingying C, Chunxue Y, Wen C. Evaluation of the efficacy of neoadjuvant chemotherapy in breast cancer by shear wave elastography. Chin Med Imaging Technol. 2016;32:71–4.
16. Santiago T, Alcacer-Pitarch B, Salvador MJ, Del Galdo F, Redmond AC, Da Silva JA. A preliminary study using virtual touch imaging and quantification for the assessment of skin stiffness in systemic sclerosis. Clin Exp Rheumatol. 2016;100:137–41.
17. Hou Y, Zhu QL, Liu H, Jiang YX, Wang L, Xu D, et al. A preliminary study of acoustic radiation force impulse quantification for the assessment of skin in diffuse cutaneous systemic sclerosis. J Rheumatol. 2015;42:449–55
18. Sun S, Yang YJ, Wang LY, Tang YJ, Qiu L, Su BH. Quantitative assessment of skin thickness using high frequency ultrasound in systemic sclerosis. J Sichuan Univ. 2018;49:453–8.
19. Yang Y, Qiu L, Wang L, Xiang X, Tang Y, Li H, et al. Quantitative assessment of skin stiffness using ultrasound shear wave elastography in systemic sclerosis. Ultrasound Med Biol. 2018;37:2507–16.

How to cite this article: Han X, Li J, Zeng F, Liu H, He Y. Differential diagnosis of basal cell carcinoma by high-resolution ultrasound elastography. Skin Res Technol. 2022;28:350–354. https://doi.org/10.1111/srt.13139